

1 Differentiated influence of the double porosity of the chalk on solute and heat transport

2
3 Richard Hoffmann^{1,2}, Pascal Goderniaux², Pierre Jamin¹, Philippe Orban¹,
4 Serge Brouyère¹, Alain Dassargues^{1*}

5
6 ¹ *Hydrogeology & Environmental Geology, Urban & Environmental Engineering, University*
7 *of Liège, Belgium*

8 ² *Geology and Applied Geology, Polytech Mons, University of Mons, Mons, Belgium*

9 * *Corresponding author (e-mail: alain.dassargues@uliege.be)*

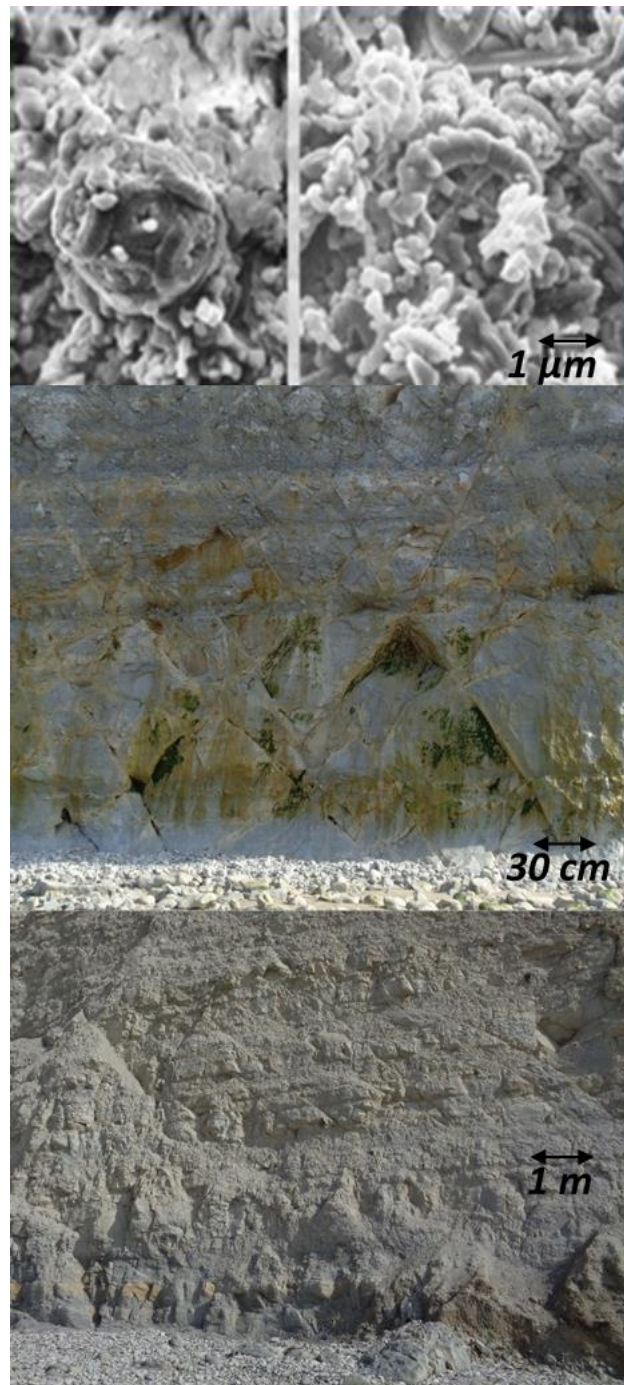
10
11
12 **Abstract:** The chalk porosity plays a decisive role in the transport of solutes and heat in
13 saturated chalk. From a geological point of view, there are at least two types of porosities: the
14 porosity of pores corresponding to the micro-spaces between the fossil coccoliths that form
15 the chalk matrix, and the porosity due to the micro- and macro-fractures (i.e., secondary
16 porosity). For groundwater flow, the fracture porosity is a determining factor at the
17 macroscopic scale. The multi-scale heterogeneity of the porous/fractured chalk is inducing
18 different effects on solute and heat transport. For solute transport considered at the
19 macroscopic scale, tracer tests have shown that the 'effective transport porosity' is
20 substantially lower than the 'effective drainable porosity'. Moreover, breakthrough curves of
21 tracer tests are showing an important influence of diffusion in a large portion of 'immobile
22 water' ('matrix diffusion') together with quick preferential advection through the fractures. For
23 heat transport, the matrix diffusion in the 'immobile water' of the chalk is hard to distinguish
24 from conduction within the saturated chalk.

25
26 Chalk aquifers are considered as excellent groundwater reservoirs (among others: Foster &
27 Milton 1974; Price 1987; Dassargues *et al.* 1988; Price *et al.* 1993; Dassargues & Monjoie
28 1993; Younger & Elliot 1995; MacDonald & Allen 2001; Nativ *et al.* 2003; William *et al.*
29 2006) but at the same time, the saturated chalk of which they are composed is one of the most
30 complex geological media due to multi-scale heterogeneity (Fig. 1). Groundwater quality
31 issues in chalk aquifers have been studied and discussed for a very long time (among others:
32 Gray & Morgan-Jones 1980; Jackson *et al.* 1984; Hallet 1998; Nativ *et al.* 1999; Goody *et*
33 *al.* 2001; Brouyère *et al.* 2004; Battle-Aguilar *et al.* 2007; Orban *et al.* 2010; Hakoun *et al.*
34 2017; Boudjana *et al.* 2019). A detailed understanding of solute transport in the chalk aquifers
35 is thus an important issue.

36 More recently, the increasing consideration of renewable energies is resulting in a huge
37 expansion of the interest on the quantification of heat transfer in partially and fully saturated
38 aquifers including chalk aquifers. Site specific values for heat transport properties/parameters
39 are needed to design shallow geothermal reservoirs and heat storage systems (i.e. Borehole
40 Thermal Energy Storage (BTES) and Aquifer Thermal Energy Storage (ATES) systems) in
41 chalk aquifers. They will influence the short-, mid- and long-term performances of the
42 systems, as well as the estimated impacts on the groundwater resources.

43 For groundwater quality as for geothermal applications, it could be very important to have a
44 realistic quantification of the highly heterogeneous groundwater flow and transport processes
45 in porous/fractured chalk formations. This information is important for modelling doublets in
46 a double porosity context (Barker *et al.* 2010). Groundwater quantity and quality assessments
47 and the subsequent protection and remediation measures should be based on a sound and

48 accurate understanding of the processes and their quantification at the scale under
49 consideration. Flow and solute transport are mainly driven by open fractures as preferential
50 paths with very high velocities, while matrix processes can also have a strong influence on
51 contamination duration (among others: Bloomfield 1996, Brouyère *et al.* 2000, Brouyère *et al.*
52 *et al.* 2004, Weiss *et al.* 2006, Massei *et al.* 2006, El Janyani *et al.* 2014, Tamayo-Mas *et al.*
53 2018, Hoffmann *et al.* 2020). Thermal storage properties could also be strongly dependent on
54 the multi-scale heterogeneity of the chalk as shown by studies recently published for other
55 geological media (Molson *et al.* 1992, Wagner *et al.* 2014, Wildemeersch *et al.* 2014,
56 Klepikova *et al.* 2016, De La Bernardie *et al.* 2019).



92
93 Fig. 1. Multi-scale heterogeneity of the chalk, from the micro-scale with coccoliths forming the chalk matrix
94 showing a pore porosity (above) towards macro-scales at which the porosity is also influenced by cracks and
95 fractures (center and below).

96 **Porosity definitions**

97 The *total porosity* is defined as:

98
99
$$n = V_v/V_t$$

100 (1)

101 where V_v is the void volume and V_t the total volume with respect to a defined representative
102 elementary volume (REV). Here, the void volume includes the pores but also all kind of
103 fractures, cracks, channels, and bedding planes. The porosity is indeed the result of various
104 processes (i.e., physical and chemical) having induced changes in the chalk throughout its
105 geological history. In geology, the terms *primary porosity* and *secondary porosity* are used to
106 describe, respectively, the initial porosity of the chalk, and the acquired additional porosity
107 due to diagenesis, fracturing or deformation, and then dissolution. This latter can often be
108 considered as the dominant process for enhancing permeability (Price 1987, Price *et al.* 1993,
109 Foster 1993). In chalks, the secondary porosity consists most often of a fracture porosity as
110 opposed to interstitial or matrix porosity. This fracture porosity can have more influence on
111 groundwater flow and the storage properties than the primary porosity. In fact, chalks can be
112 considered as dual porosity media with fracture network and matrix porosities, even if a part
113 of this matrix porosity can be reduced by cementing materials in the pore spaces.

114 The definition of porosity implies conceptually that a given volume of the chalk is considered,
115 which is big enough to yield a value considered as representative at that scale. In practice, the
116 REV concept is always implicitly considered even though this is not necessarily
117 acknowledged (de Marsily 1986). Behind this concept lies the fact that an equivalent value is
118 used (Bachmat and Bear 1986, Bear and Verruijt 1987) that is the result of a homogenization
119 process at that REV scale. The size of the later is chosen essentially according to the aims of
120 the study.

121 In many different aquifers, but especially in chalk aquifers, observations at the scale of lab
122 tests (up to a few decimetres) or at the scale of field tests (e.g., pumping tests) imply that a
123 part of the groundwater in the aquifers can be considered as immobile in the pores of the
124 matrix. In all textbooks about hydrogeology an effective porosity is distinguished from the
125 total porosity.

126 In saturated conditions and for groundwater flow problems, an *effective porosity* is usually
127 defined as the drainable porosity under the in-situ pressure conditions:

128
129
$$n_e = V_m/V_t$$

130 (2)

131 where V_m is the volume of mobile water in the REV. This corresponds to the specific yield
132 (S_y). This specific yield or drainable effective porosity gives also a reliable value for the
133 storage coefficient in unconfined aquifers (i.e., as consolidation effects can be neglected in
134 unconfined conditions).

135 If solute transport is considered, it remains difficult to know accurately which part of the
136 saturated porosity is occupied by mobile water, on which the transport velocity is based
137 (Dassargues 2018). In particular, in aquifers where a fracture porosity is usually lower or around
138 1 %, very rapid transport (advection) velocities are observed (Worthington 2015). On the basis
139 of all observations from tracer tests and contaminations, distinction must be made
140 systematically between the effective drainable porosity and an effective transport porosity
141 which takes typically a lower value than the former one (Hallet & Dassargues 1998, Brouyère

142 *et al.* 2000, Payne *et al.* 2008, Hadley & Newell, 2014). In addition, Worthington *et al.* (2019)
143 have recently demonstrated that the transient nature of effective porosity and specific yield is
144 of importance for an unconfined chalk aquifer, highlighting that these values should not
145 necessarily be treated as similar, time-invariant values.

146 The advection velocity is defined as:

147

148

$$v_a = \mathbf{q}/n_m \quad (3)$$

149

150 where \mathbf{q} is the groundwater Darcy flux, and n_m is the *effective transport porosity* (Dassargues
151 2018). This later is in theory very dependent on what is actually defined as mobile and
152 immobile groundwater in the REV. In practice however, if experimental results (i.e., pumping
153 tests and tracer tests results) have to be reproduced by model results, a lower value for the
154 effective transport porosity is to be chosen than for the effective drainable porosity.

155 Especially in the chalk, if the Darcy flux were divided by the total porosity n (or even by the
156 effective drainable porosity n_e), this would lead to a kind of averaged velocity which can be
157 misleading (i.e., leading to underestimation of actual velocities). However, one can argue that
158 this could be partially and artificially compensated in models by considering larger values of
159 the longitudinal dispersivity, but it is also misleading as it only counterbalances a correlation
160 between parameters and not improve the model conceptualisation towards an accurate
161 parameterisation (Dassargues 2018).

162

163 **Dual porosity and hydraulic conductivity of chalk**

164 The dual porosity concept, with micro-pores in the solid porous matrix and macro-pores
165 corresponding to fractures or bedding, was already considered by Gerke & van Genuchten
166 (1993). If it is applied at larger scale, subzones of low and high hydraulic conductivity also
167 form a dual permeability medium (Dassargues 2018).

168 Indeed, a dual or triple porosity of the chalk could be considered as a result of the geological
169 processes having led to these pores, micro- and macro-fractures (Fig. 1 and Fig. 2). The
170 influence of this multi-scale heterogeneity can be considered differently in function of the
171 studied processes (i.e., groundwater flow, solute transport and heat transport). In each case,
172 the parameter values are considered at a given scale (i.e., the scale of the REV) depending on
173 the problem to be solved.

174

175

176

177

178

179

180

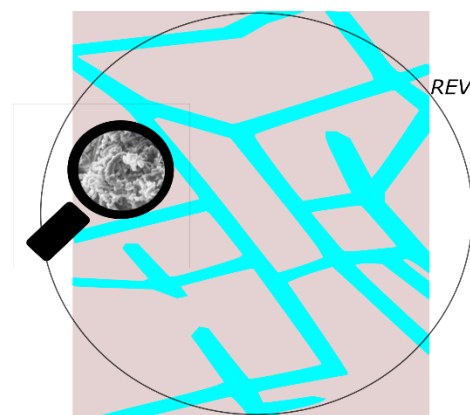
181

182

183

184

185



186

186 Fig. 2. Porosity of the pores in the matrix made up of coccoliths and fracture network porosity at the
187 macroscopic REV scale.

188

189 As an example, if only groundwater flow properties are considered in the chalk aquifer of
 190 Hesbaye (Cretaceous chalks of the Maastrichtian and Campanian ages of the Geer basin in
 191 Belgium), different values (see below) were found according to the considered size of the
 192 REV (Dassargues 2018).

193 At the *microscopic scale* (up to a few centimeters), one considers essentially the matrix of a
 194 chalk sample. Aggregated coccolith fossils of a few microns are forming this chalk matrix.
 195 The measured porosity may vary depending on localized calcium carbonate (CaCO₃)
 196 precipitation. The overall spatial distribution of voids seems relatively homogeneous in the
 197 samples of a few centimeters, so they are apparently adequate REV's to measure a reliable
 198 pore porosity. The following values have been measured: $n = 0.40 - 0.42$ and $n_e = 0.35$.
 199 Consequently, the hydraulic conductivity values are quite low $K \cong 1.0 \cdot 10^{-8}$ (m/s).

200 At the *macroscopic scale* (up to a few decimeters), any REV actually includes conjugate
 201 micro-fractures networks (or micro-fractures) and chalk layering. The effective drainable
 202 porosity (i.e., to be considered for a groundwater flow through this REV and influencing the
 203 hydraulic conductivity at this scale) is now strongly dependent the porosity of these micro-
 204 fractures: $n = 0.42 - 0.45$ and $n_e = 0.01 - 0.03$. Accordingly, larger values of hydraulic
 205 conductivity are found with $1.0 \cdot 10^{-5} \leq K \leq 1.0 \cdot 10^{-4}$ (m/s).

206 At the *megascopic scale* (scale of field tests such as pumping tests, up to a few hundred
 207 meters), it is observed (through interpretation of tests and inverse modelling) that
 208 'homogenization' in a large REV ensures that all fractures, faults and discontinuities should
 209 be considered as interconnected, which increases the effective porosity and the hydraulic
 210 conductivity values: $n = 0.42 - 0.45$ and $n_e = 0.05 - 0.10$; $1.0 \cdot 10^{-4} \leq K \leq 1.0 \cdot 10^{-3}$
 211 (m/s).

212 Now if solute or heat advection is considered, the n_m values are systematically lower than the
 213 n_e values, representing a more accurate assessment of the actual mobile water volume for
 214 advective mass transport. For example, for solute transport, on the basis of 47 different tracer
 215 tests in Belgian unconfined chalk aquifers performed for delineation of protection zones
 216 around pumping wells, the arithmetic mean, geometric mean and median values for n_m were
 217 found to be 0.0187, 0.0058, and 0.008, respectively (Briers *et al.* 2017).

218 In summary, this concept of dual porosity is at the origin mostly influenced by the chalk
 219 geological conditions and history. Its relative importance for possible consideration in the
 220 quantification of solute and heat processes is largely dependent on the scope of the study and
 221 the associated scale of consideration.

222

223 **Solute transport in chalk accounting for matrix diffusion/immobile water effect**

224 Adding the contribution of the different solute mass processes, the solute conservation
 225 equation for mobile groundwater can be written for a REV in aquifers (Dassargues 2018):
 226

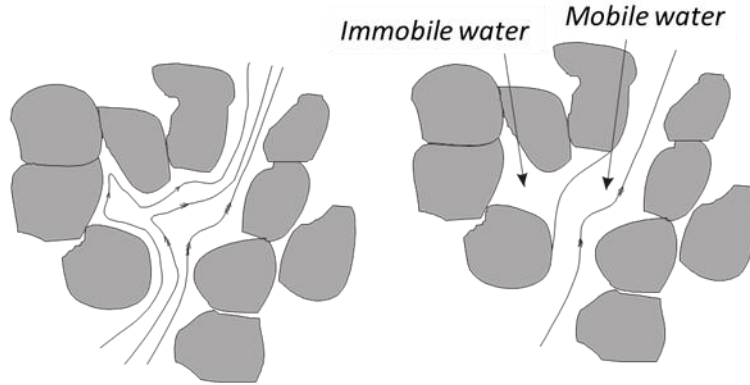
227

$$R \frac{\partial C}{\partial t} = - \mathbf{v}_a \cdot \nabla C + \nabla \cdot (\mathbf{D}_h \cdot \nabla C) - R\lambda C - \frac{q_s}{n_m} (C - C_s) \quad (4)$$

228

229 where C is the volume concentration (kg/m³) in the mobile groundwater, \mathbf{D}_h is the
 230 hydrodynamic dispersion tensor (m²/s) including the mechanical dispersion and the diffusion
 231 in the mobile water, R is the retardation factor due to adsorption-desorption processes (-), λ is
 232 a first-order (linear) decay constant (s⁻¹), q_s is the source/sink volumetric flow rate per unit
 233 volume of porous medium (s⁻¹) flowing into ($q_s > 0$) or flowing out from ($q_s < 0$) the control
 234 volume and C_s is the associated concentration (kg/m³). In this equation, diffusion is
 235 considered only in the mobile water fraction of the saturated media.

236 In reality, diffusion occurs between mobile water and immobile water as a result of solute
 237 concentration differences. Especially in a porous/fractured chalk, the concentration (C) first
 238 rises in the very mobile groundwater in the fractures (Fig. 3). In contact with the immobile
 239 water at a concentration (C_{im}) in the matrix pores, diffusion occurs (i.e., assuming $C > C_{im}$).
 240 On the contrary, when the peak in mobile water concentration C has passed, back diffusion
 241 can take place from the immobile into the mobile water (i.e., assuming $C < C_{im}$).
 242



253 Fig. 3 Schematic view of the highly mobile water in fractures or macro-pores and the quasi immobile water in
 254 the pores of the chalk.

256 This immobile water effect on the solute transport is often referred to as ‘matrix diffusion’ in
 257 the literature (Rasmusen & Neretnieks 1981, Wood *et al.* 1990, Carrera *et al.* 1998). It was
 258 detected by tracer tests showing longer tailing of the breakthrough curve (BTC). One of the
 259 way to take this matrix diffusion into account is to express a classical linear exchange
 260 relationship as (Coats & Smith 1964, Bear & Verruijt 1987, Brouyère 2001):
 261

$$f_m^{im} = \alpha_d^m (\rho C - \rho_{im} C_{im}) \quad (5)$$

264 where f_m^{im} is the diffusive solute mass flux ($\text{kg}/\text{m}^3\text{s}$) from mobile to immobile water (or vice-
 265 versa), ρ and ρ_{im} are the density of mobile and immobile water respectively, α_d^m is defined
 266 as the matrix diffusion coefficient or immobile water diffusion coefficient (s^{-1}), similar to a
 267 diffusion coefficient (m^2/s) divided by a surface area (m^2) intended to describe the mobile
 268 water - immobile water contact area. This flux could be added to the solute conservation
 269 equation expressed for the mobile water in the REV (equation 4). In practice, to obtain the net
 270 gain or loss of solute mass in the mobile water at each time step (i.e., dual-domain mass
 271 transfer), a solute mass balance equation in the immobile water must also be considered.
 272 Values for the matrix diffusion coefficient (α_d^m) are inferred from lab and field tracer tests
 273 results and diffusion coefficient values. As studied by Brouyère (2001), this value can have a
 274 crucial influence on the simulated BTC (Fig. 4).
 275

276 A few examples of BTC from tracer tests performed in the unconfined chalk aquifer of Hesbaye
 277 (Geer basin, Belgium) show the wide diversity of the obtained BTC in function of the local
 278 multi-scale heterogeneity of the chalk (Fig. 5).
 279
 280
 281
 282
 283
 284

285
286
287
288
289
290
291
292
293
294
295
296
297
298
299
300
301
302
303
304
305
306
307
308
309
310
311
312
313
314
315
316
317
318
319
320
321
322
323
324
325
326
327
328
329
330
331
332
333
334

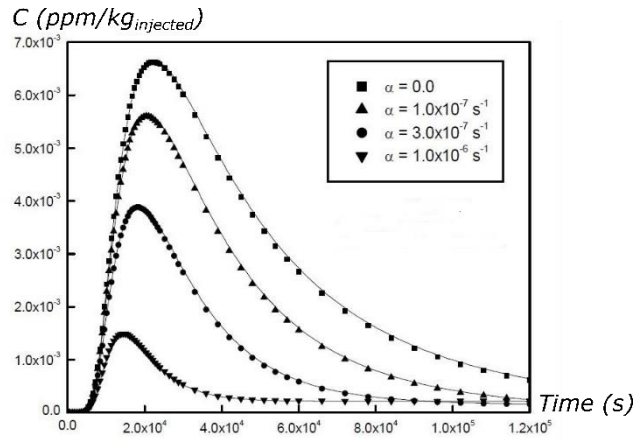


Fig. 4 Calculated BTCs in a pumping well for a saturated chalk with 30 % of immobile water and $n_m = 1\%$, with different values for the matrix diffusion coefficient (from Brouyère 2001).

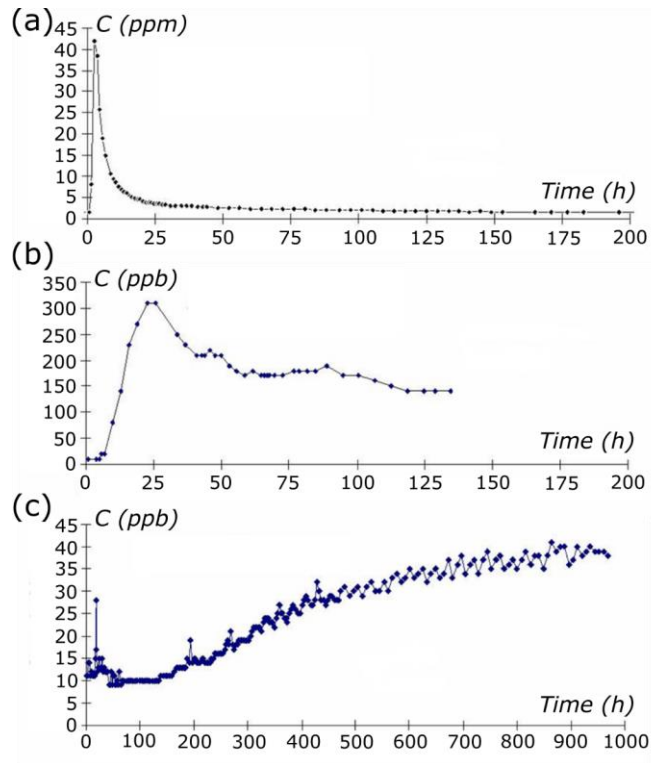


Fig. 5 Examples of measured breakthrough curves for different tracer tests tracers performed in in the unconfined chalk aquifer of Hesbaye (Geer basin in Belgium) showing the diversity of the solute transport behaviour.

More details about the tracing conditions (Hallet 1998) and interpretation:

(a) 52 kg of potassium, injected (in depth-averaged conditions) during 2h at a distance of 93 m from the pumping well with a discharge rate of $9 \text{ m}^3/\text{h}$. Local hydraulic conductivity values were assessed between 4.0 and $20.0 \cdot 10^{-4} \text{ m/s}$ in the fractured zones and about $8.5 \cdot 10^{-5} \text{ m/s}$ in the less fractured chalk from pumping tests interpretation. The clear advection dominated solute behaviour with a moderate tailing is due to preferential flow through open fractures or conduits.

(b) 22.9 kg of iodide, injected (in depth-averaged conditions) during 9h45 at a distance of 54 m from a drainage gallery (BTC was measured in the gallery). Local hydraulic conductivity values were assessed between 3.0 and $10.0 \cdot 10^{-4} \text{ m/s}$ in the fractured zones and between 0.1 and $8.0 \cdot 10^{-5} \text{ m/s}$ in the less fractured chalk from pumping tests interpretation. The long tailing with relatively high concentrations clearly shows a strong immobile water effect with occurrence of matrix diffusion and back-diffusion.

(c) 4.1 kg of lithium, injected (in depth-averaged conditions) during 30h at a distance of 110 m from the pumping well with a discharge rate of $4.4 \text{ m}^3/\text{h}$. Local hydraulic conductivity values are assessed between 1.0 and $10.0 \cdot 10^{-3} \text{ m/s}$ in the fractured zones and between 0.3 and $1.0 \cdot 10^{-5} \text{ m/s}$ in the less fractured chalk from pumping tests interpretation. The atypical BTC can be interpreted as showing a limited first advection arrival at very short times corresponding to a preferential flowpath through a

335 fractured zone detected previously by geophysics, and a quite delayed second peak due to the solute
 336 pathway through the less fractured chalk matrix.

337

338 Heat transport in chalk

339 Heat can be transported through both the pore/fracture space and the solid matrix of the chalk,
 340 whereas solutes in groundwater are transported only through the pores and fractures. The
 341 main processes for heat transfer in a saturated chalk are thermal conduction, advection and
 342 dispersion. The corresponding heat conservation equation can be written:

343

$$344 \quad \frac{\partial \rho_b c_b T}{\partial t} = -\nabla \cdot [\rho_w c_w \mathbf{q} T - (\lambda_b + c_b \rho_b \mathbf{D}) \cdot \nabla T] + Q_T \quad (6)$$

345

346 where λ_b is the heat (or thermal) conductivity (W/(m²K)) of the bulk saturated chalk, ρ_b is the
 347 bulk density (kg/m³), c_b is the bulk heat capacity (J/(kg²K)) ($\rho_b c_b$ is the bulk volumetric heat
 348 capacity J/(m³K)), ρ_w is the water density (kg/m³), c_w is the water heat capacity (J/(kg²K))
 349 ($\rho_w c_w$ is the water volumetric heat capacity in J/(m³K)), \mathbf{q} is the total water flux vector (m/s)
 350 from Darcy's law and including the possible temperature effect on the water density and
 351 viscosity (natural convection), \mathbf{D} is the thermal dispersion tensor (m²/s), ∇T the temperature
 352 gradient (°K/m), Q_T is the heat source (if $Q_T > 0$) or sink (if $Q_T < 0$) term.

353 In aquifers, most often, the thermal dispersion is considered as negligible compared to the
 354 thermal conduction term and compared to the advection-convection term (Anderson 2005,
 355 Irvine *et al.* 2015). Then, the equation is accordingly simplified and divided by the bulk
 356 volumetric heat capacity ($\rho_b c_b$) to obtain (Dassargues 2018):

357

$$358 \quad \frac{\partial T}{\partial t} = -\nabla \cdot \left[\frac{\rho_w c_w}{\rho_b c_b} \mathbf{q} T - \frac{\lambda_b}{\rho_b c_b} \nabla T \right] + Q_T / (\rho_b c_b) \quad (7)$$

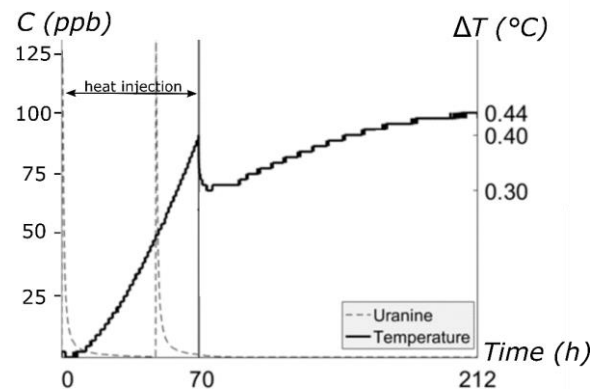
359

360 where the coefficient $\lambda_b / (\rho_b c_b)$ is named thermal diffusivity (m²/s) and the term $Q_T / (\rho_b c_b)$
 361 (°K/s) can also be understood as the temperature associated with a groundwater flux entering
 362 or exiting 1 m³ of the domain

363 For heat transport the 'effective heat transport porosity' could probably be considered as equal
 364 to the 'effective solute transport porosity' in the advection term. On the contrary, the
 365 'diffusive term' in the heat transport equation corresponds to conduction (as heat dispersion is
 366 often considered as to be neglected with regards to conduction) that occurs in solid matrix and
 367 both mobile and immobile water. So, the total porosity is required to assess the values of the
 368 bulk saturated chalk matrix heat capacity (c_b) and density (ρ_b) that are considered in the heat
 369 transport equation. Conduction is actually boosted by the temperature difference between the
 370 mobile water and the immobile water, and also between the mobile water and the solid matrix.
 371 These effects are fully included in the diffusive term of the heat solute transport equation
 372 (equation 7). This last term is most often three orders of magnitude higher than a solute
 373 diffusion term in a solute transport equation. Thus, looking at equation (7), the immobile
 374 water effect on the heat transfer is clearly integrated in the thermal diffusivity term describing
 375 conduction in the bulk saturated media.

376 Usual values for bulk thermal conductivities (λ_b) are comprised between 0.5 and 2.5 (W m⁻¹
 377 °K⁻¹) for a dry chalk and between 0.57 and 0.60 for water. Usual values for bulk heat
 378 capacity (c_b) and volumetric heat capacity ($\rho_b c_b$) for a dry chalk are about 0.90 10³ (J kg⁻¹°K⁻¹)
 379 and 2.2 – 2.25 10⁶ (J m⁻³°K⁻¹) respectively, and 4.18 10³ (J kg⁻¹°K⁻¹) and 4.18 10⁶ (J m⁻³°K⁻¹)
 380 for water.

381 An example of a temperature BTC from a tracer test performed in a continuous chalk fracture
 382 isolated between packers is shown in Fig. 6. The injection well (i.e. with the isolated fracture
 383 between packers at 35 m of depth) is located at 7.55 meters from the pumping well in the
 384 unconfined chalk of the Mons basin (Belgium) (more details in the Fig. 6 legend). It shows
 385 clearly heat advection and then the combined effect of the conduction and possibly matrix
 386 diffusion in the delayed answer of heat evolution with time. As long as the injection of hot
 387 water is in progress the curve rises showing essentially advection, but as soon as the injection
 388 is stopped, apart from a small and temporary drop in temperature (due to the drop in
 389 temperature in the fracture itself), a new but slow temperature rise is observed by conduction
 390 and possibly matrix diffusion (Fig. 6). Interestingly, the finally measured temperature change
 391 in the recovery well is 0.44 °C, and thus already 10 % higher than the peak measured during
 392 the active injection of hot water. Due to the stop of the hot water injection, but the ongoing
 393 pumping in Pz1 during this period, heat stored in the rock matrix around the injection well
 394 and around the fractures between the injection and pumping wells, is probably progressively
 395 released from the rock matrix to the colder water circulating in the fractures towards the
 396 pumping well. In contrast, the comparison with the solute (uranine) behavior is striking with a
 397 very quick advection of solute, as expected, since the injection was performed in the fracture
 398 between packers.



411
 412 Fig. 6 Observed concentration of uranine and temperature change at a recovery pumping well 7.2 m³/h located
 413 at a 7.55 m distance from the injection well. Both wells are crossing an identified sub-horizontal fracture
 414 connecting them at a depth of 35 m. A 70 h injection of hot water ($\Delta T = + 40$ °C) was complemented by two 10
 415 minutes uranine pulse injections within an inflatable double packer system isolating the sub-horizontal chalk
 416 fracture of interest. The uranine tracer was injected simultaneously with the start of the hot water injection.
 417 During the first period (i.e., continuous hot water injection period during the first 70 h), both uranine injections
 418 show first arrival times of about 10 minutes at the recovery well. In contrast, the first measured temperature
 419 increases of 0.01 °C is observed after 12.5 h. The followed observed heat increasing increments are always 0.01
 420 °C and the time between two increments is getting shorter till the peak is reached. After 70 h of hot water
 421 injection, the measured temperature change in the recovery well is 0.40 °C, far from having reached a steady-
 422 state temperature value. After the stop of hot water injection, the temperature decreases first rapidly to 0.33 °C,
 423 before a further temperature rebound.

424
 425 **Conclusion and perspectives**
 426 In chalk aquifers, it could be particularly recommended to distinguish between the different
 427 kinds of porosity. A pumping test in an unconfined chalk aquifer in transient conditions
 428 allows to deduce interpreted values for hydraulic conductivity and effective drainable porosity
 429 (specific yield), while a tracer test (with an ideal solute tracer) would confirm that this latter is

430 not the adequate porosity to calculate advection groundwater velocity. In reality, a systematic
431 difference is observed between the portion of mobile water for flow calculation and the
432 portion of mobile water actually transporting the solute by advection. This is particularly true
433 in chalk aquifers showing a multi-scale heterogeneity with pores and various micro- and
434 macro-fractures.

435 For solute transport, the matrix diffusion in the immobile water should be accounted for to
436 obtain a reasonably realistic quantification and characterisation. For heat transport on the
437 contrary, possible matrix diffusion is masked and thus can be included in thermal conduction
438 that is active through both the pore/fracture space and the solid matrix of the chalk.

439 Finally, determining the breakthrough curve of a solute contaminant at a given pumping well
440 (i.e., mainly influenced by advection, dispersion and matrix diffusion) is completely another
441 problem than assessing efficiency of an ATEs geothermal system that will be mainly
442 dependent on advection and conduction). Each process should be investigated and calculated
443 with its corresponding specific behaviour in the multi-scale heterogeneity context of the
444 chalk. This is requiring a lot of characterisation work involving well designed in situ solute
445 and heat tracer tests.

446

447 **Acknowledgement**

448 The test linked to the joint heat-solute injection (Fig. 6) was part of the PhD research of R.
449 Hoffmann as ESR in the ITN ENIGMA, which received funding from European Union's
450 Horizon 2020 research and innovation programme under the Marie Skłodowska-Curie Grant
451 Agreement N°722028. The test site was partly funded by the Belgian “Fonds de la Recherche
452 Scientifique” - FNRS under Grant n° J.0115.15. The authors thank the editor and the
453 reviewers for the positive and fruitful discussion and their suggestions of corrections.

454

455 **Data Availability**

456 The data set of the joint heat-solute experiment is stored on the H+ Network database
457 (<http://hplus.ore.fr/en/hoffmann-et-al-2020-hydrogeology-of-the-chalk-data>). The access will
458 be free 6 months after publication. The authors express their special thanks to N. Guihéneuf by
459 assisting the data upload to the H+ database.

460 **References**

- 461 Anderson, M.P. 2005. Heat as a ground water tracer. *Groundwater* 43(6): 951-968.
- 462 Bachmat, Y. & Bear, J. 1986. Macroscopic modelling of transport phenomena in porous
463 media, part 1: The continuum approach *Transport in Porous media* (1) 213-240.
- 464 Barker, J. A. 2010. Modelling doublets and double porosity. *Q. J. Eng. Geol. and*
465 *Hydrogeology* 43(3), 259 - 268.
- 466 Batlle-Aguilar, J., Orban, Ph., Dassargues, A. & Brouyère, S. 2007. Identification of
467 groundwater quality trends in a chalky aquifer threatened by intensive agriculture, *Hydrogeol.*
468 *J.* 15: 1615-1627.
- 469 Bear, J. & Verruijt, A. 1987. *Modeling groundwater flow and pollution*. Dordrecht: Reidel
470 Publishing Company.
- 471 Bloomfield J. 1996. Characterisation of hydrogeologically significant fracture distributions in
472 the Chalk: an example from the Upper Chalk of southern England. *J. Hydrol.* 184: 355-379.
- 473 Boudjana Y., Brouyère S., Jamin P., Orban Ph., Gasparella, D. & Dassargues, A. 2019.
474 Understanding groundwater mineralization changes of a Belgian chalky aquifer in the
475 presence of 1,1,1-trichloroethane degradation reactions. *MDPI Water* 11(10)
476 10.3390/w11102009.
- 477 Briers, P., Dollé, F., Orban, P., Piront, L. & Brouyère, S. 2017. Etablissement des valeurs
478 représentatives par type d'aquifère des paramètres hydrogéologiques intervenant dans
479 l'Évaluation des risques pour les eaux souterraines en application du Décret du 5 décembre
480 2008 relatif à la Gestion des Sols (*in French*). University of Liège - GEOLYS final report.
481 SPW/DGO3, Walloon Region (Belgium).
- 482 Brouyère, S. 2001. Etude et modélisation du transport et du piégeage des solutés en milieu
483 souterrain variablement saturé (Study and modelling of transport and retardation of solutes in
484 variably saturated media, in French), PhD Thesis, University of Liege.
- 485 Brouyère, S., Dassargues, A., Therrien R. & E. Sudicky. 2000. Modelling of dual porosity
486 media: comparisons of different techniques and evaluation of the impact on plume transport
487 simulations. In: Stauffer F., Kinzelbach W. Kovar, K and Hoehn E. (eds) *Proc. of the*
488 *ModelCARE'99 Conference*, Zürich, IAHS Publ. 265: 22-27.
- 489 Brouyère, S., Carabin, G. & Dassargues, A. 2004. Climate change impacts on groundwater
490 reserves: modelled deficits in a chalky aquifer, Geer basin, Belgium, *Hydrogeol. J.* 12(2):
491 123-134.
- 492 Coats, K.H. & Smith, B.D. 1964. Dead-end pore volume and dispersion in porous media. *Soc.*
493 *Pet. Eng. J.*: 73-84.
- 494 Carrera, J., Sánchez-Vila, X., Benet, I., Medina, A., Galarza, G. et Guimera J. 1998. On
495 matrix diffusion: formulations, solution methods and qualitative effects. *Hydrogeol J.* 6: 178-
496 190.
- 497 Dassargues, A. 2018. *Hydrogeology - groundwater science and engineering*. CRC Press.
- 498 Dassargues A., Radu J.P. & Charlier R. 1988. Finite elements modelling of a large water table
499 aquifer in transient conditions. *Adv. Water Res.* 11(2): 58-66.
- 500 Dassargues A. & Monjoie A. 1993. Chalk as an aquifer in Belgium. In: Downing, R.A., Price,
501 M. Jones, G.P. (eds.) *The hydrogeology of the chalk of north-west Europe*. Clarendon Press,
502 Oxford. 153-169.
- 503 De La Bernardie, J., Bour, O., Guihéneuf, N., Chatton, E., Longuevergne, L. & Le Borgne, T.
504 2019. Dipole and convergent single-well thermal tracer tests for characterizing the effect of
505 flow configuration on thermal recovery. *Geosciences* 9(10): 440.

506 de Marsily, G. 1986. *Quantitative hydrogeology: groundwater hydrology for engineers*.
507 Academic Press.

508 El Janyani, S., Dupont, J., Massei, N., Slimani, S. & Dörfliger, N. 2014. Hydrological role of
509 karst in the chalk aquifer of Upper Normandy, France. *Hydrogeol. J.* 22: 663-677.

510 Foster, S.S.D. & Milton, V.A. 1974. The permeability and storage of an unconfined chalk
511 aquifer. *Hydrol. Sci. Bull.* 19: 485-500.

512 Foster, S.S.D. 1993. The Chalk aquifer - its vulnerability to pollution. *In: Downing, R.A.,*
513 *Price, M. Jones, G.P. (eds.) The hydrogeology of the chalk of north-west Europe.* Clarendon
514 Press, Oxford. 93-112.

515 Gerke, H.H. & van Genuchten, M.Th. 1993. A dual-porosity model for simulating the
516 preferential movement of water and solutes in structured porous media. *Water Resources*
517 *Research* 29(2): 305-319.

518 Goody, D., Bloomfield, J., Chilton, P., Johnson, A. & Williams, R. 2001. Assessing
519 herbicide concentrations in the saturated and unsaturated zone of a chalk aquifer in Southern
520 England. *Groundwater* 39: 262-271.

521 Gray, E.M. & Morgan-Jones, M. 1980. A comparative study of nitrate levels at three adjacent
522 groundwater sources in a chalk catchment area west of London. *Groundwater* 18: 159-167.

523 Hadley, P.W. & Newell, C.J. 2014. The new potential for understanding groundwater
524 contaminant transport. *Groundwater* 52(2): 174-186.

525 Hakoun V., Orban Ph., Dassargues A. & Brouyère S. 2017. Factors controlling spatial and
526 temporal patterns of multiple pesticide compounds in groundwater (Hesbaye chalk aquifer,
527 Belgium). *Env. Pollution* 223: 185-199.

528 Hallet, V. 1998. Etude de la contamination de la nappe aquifère de Hesbaye par les nitrates (in
529 French). PhD thesis, University of Liège, Belgium.

530 Hallet V. & Dassargues A. 1998. Effective porosity values used in calibrated transport
531 simulations in a fissured and slightly karstified chalk aquifer. *In: Herbert, M. & Kovar, K.*
532 *(eds.) Groundwater Quality 1998, Tübinger Geowissenschaftliche Arbeiten (TGA), C36: 124-*
533 *126.*

534 Hoffmann R., Goderniaux P., Jamin P., Chatton E., Labasque T., Le Borgne T. & Dassargues,
535 A. 2020. Continuous dissolved gas tracing of fracture-matrix exchanges. *Geophysical*
536 *Research Letters* 47(17) e2020GL088944.

537 Irvine, D.J., Simmons, C.T., Werner, A.D. & Graf, T. 2015. Heat and solute tracers: how do
538 they compare in heterogeneous aquifers? *Groundwater* 53(S1): 10-20.

539 Jackson, D. & Lloyd, J.W. 1984. An integrated hydrochemical approach to deduce the
540 response of an aquifer system during its history of abstraction. *Groundwater* 22: 735-745.

541 Klepikova M., Wildemeersch S., Jamin P., Orban Ph., Hermans T., Nguyen F., Brouyere S. &
542 Dassargues A. 2016. Heat tracer test in an alluvial aquifer: field experiment and inverse
543 modelling. *J. Hydrol.* 540: 812-823.

544 MacDonald, A.M. & Allen, D.J. 2001. Aquifer properties of the Chalk of England. *Q. J. Eng.*
545 *Geol. Hydrogeol.* 34: 371-384.

546 Massei, N., Wang, H.Q., Field, M.S., Dupont, J.P., Bakalowicz, M. & Rodet, J. 2006.
547 Interpreting tracer breakthrough tailing in a conduit-dominated karstic aquifer. *Hydrogeol. J.*
548 14: 849-858.

549 Molson, J. W., Frind, E. O. & Palmer, C. D. 1992. Thermal energy storage in an unconfined
550 aquifer: 2. Model development, validation, and application. *Water Resour. Res.* 28(10): 2857-
551 2867.

552 Nativ, R., Adar, E. & Becker, A. 1999. Designing a monitoring network for contaminated
553 ground water in fractured chalk. *Groundwater* 37: 38-47.

554 Nativ, R., Adar, E., Assaf, L. & E. Nygaard. 2003. Characterization of the hydraulic
555 properties of fractures in chalk. *Ground Water* 41: 532-543.

556 Orban, P., Brouyère, S., Batlle-Aguilar, J., Couturier, J., Goderniaux, P., Leroy, M.,
557 Malozewski, P. & Dassargues, A. 2010. Regional transport modelling for nitrate trend
558 assessment and forecasting in a chalk aquifer, *J. Cont. Hydrol.* 118: 79-93.

559 Payne, F.C., Quinnan, A. & Potter. S.T. 2008. *Remediation hydraulics*. Boca Raton: CRC
560 Press/ Taylor & Francis.

561 Price, M. 1987. Fluid flow in the Chalk of England. *Geol. Soc. Spec. Publ.* 34: 141-156.

562 Price, M., Downing R.A. & Edmunds, W. 1993. The chalk as an aquifer. *In: Downing, R.A.,*
563 *Price, M. Jones, G.P. (eds.) The hydrogeology of the chalk of north-west Europe*. Clarendon
564 Press, Oxford. 35-58.

565 Rasmuson, A. & Neretnieks, I. 1981. Migration of radionuclides in fissured rocks: the
566 influence of micropore diffusion and longitudinal dispersion. *J Geophys Res* 86: 3749-3758.

567 Tamayo-Mas, E., Bianchi, M. & Mansour, M. 2018. Impact of model complexity and multi-
568 scale data integration on the estimation of hydrogeological parameters in a dual-porosity
569 aquifer. *Hydrogeol. J.* 26: 1917-1933.

570 Wagner, V., Li, T., Bayer, P., Leven, C., Dietrich, P. & Blum, Ph. 2014. Thermal tracer
571 testing in a sedimentary aquifer: field experiment (Lauswiesen, Germany) and numerical
572 simulation. *Hydrogeol J* 22: 175-187.

573 Weiss, M., Rubin, Y., Adar, E. & Nativ, R. 2006. Fracture and bedding plane control on
574 groundwater flow in a chalk aquitard. *Hydrogeol. J.* 14: 1081-1093.

575 Wildemeersch S., Jamin P., Orban Ph., Hermans T., Klepikova M., Nguyen F., Brouyère S. &
576 Dassargues A. 2014. Coupling heat and chemical tracer experiments for estimating heat
577 transfer parameters in shallow alluvial aquifers. *J. Cont. Hydrol.* 169: 90-99.

578 Williams, A., Bloomfield, J., Griffiths, K. & Butler, A. 2006. Characterising the vertical
579 variations in hydraulic conductivity within the Chalk aquifer. *J. Hydrol.* 330: 53-62.

580 Wood, W.W., Kraemer, T.F. & Hearn, P.P. 1990. Intergranular diffusion: an important
581 mechanism influencing solute transport in classic aquifers? *Science* 247:1569-1572

582 Worthington, S.R.H. 2015. Diagnostic tests for conceptualizing transport in bedrock aquifers.
583 *Journal of Hydrology* 529: 365-372.

584 Worthington, S. R., Foley, A. E., & Soley, R. W. 2019. Transient characteristics of effective
585 porosity and specific yield in bedrock aquifers. *Journal of Hydrology* 578: 124129.

586 Younger, P.L. & Elliot, T. 1995. Chalk fracture system characteristics: implications for flow
587 and solute transport. *Q. J. Eng. Geol.* 28: S39-S50.